

# Dynamical Systems Analysis of $f(R, \mathcal{G})$ Cosmological Model with Dark Sector Coupling

Shivani Sharma,\* R. Chaubey†

Centre for Interdisciplinary Mathematical Sciences

Institute of Science, Banaras Hindu University

Varanasi, Pin 221005, India

August 28, 2024

## Abstract

In this article, we examine the dynamical system of  $f(R, \mathcal{G})$  gravity model. This  $f(R, \mathcal{G})$  model framework is composed of the interactions between dark matter and scalar field through the linear coupling term. The key objective of present study is to describe the cosmological viability of modified gravity theory formulated with the  $f(R, \mathcal{G})$  gravity. We transform the cosmological equations into an autonomous system of ordinary differential equations by suitable transformation of variables. The  $f(R, \mathcal{G})$  model governed by  $f(R, \mathcal{G}) = \alpha R^m + \beta \mathcal{G}^n$  has been investigated in detail to characterize the stability properties of the critical points of the autonomous system. The model may explain the late-time accelerating universe expansion corresponding to the attractor in model. Depending on the effective equation of state parameter values corresponding to the critical points, we study the observational viability of model using low-redshift observational data such as the observational Hubble data and Pantheon data. Furthermore, we investigate the effects of parameters by using the effective equation of state parameter and statefinder diagnostics.

**Keywords:** FRW Cosmological model, Dynamical systems, Dark energy, Coupling parameter,  $f(R, \mathcal{G})$  gravity.

---

\*shivani1506@bhu.ac.in

†corresponding author: R Chaubey, yahoo\_raghav@rediffmail.com, rchaubey@bhu.ac.in

# 1 Introduction

One of the most complex and interesting problem in the physical sciences is concerned with the creation and evolution of the universe. The General theory of relativity (GTR) is the most prominent theory for characterizing the universe and it had completely changed the perception of physicists about the universe. The GTR may explain the cosmic acceleration of the universe at late times, which is also supported by recent data such as the Supernovae type Ia (SNe Ia) [1,2], direct measurements of the Hubble parameter [3] along with the cosmic microwave background radiation (CMBR) [4] and the baryonic acoustic oscillations (BAO) [5]. The cosmic acceleration is due to the negative pressure caused by an enigmatic force known as the dark energy. According to the standard model of cosmology called as the  $\Lambda$ -cold dark matter ( $\Lambda$ CDM) model, presently, the evolution of the Universe is ruled by two dominant factors named as the dark matter and dark energy. These two factors constitutes around 95% energy of the Universe. This model suggests that after the Big Bang, the universe went through inflation followed by an era dominated by radiation and matter, which then led to a phase of accelerated expansion dominated by dark energy [6–8]. However, this widely accepted model also faces challenges such as the cosmological constant problem and coincidence problem [9–12].

One of the approaches to alleviate the cosmological problems such as the cosmic coincidence problem is the interacting dark energy cosmology. On using many available cosmological observations, it has been analyzed that there is a possibility of interactions involving dark Matter and dark Energy [13,14]. These kind of models are primarily based on the idea that the dark matter and dark energy may non-gravitationally interact with each other. The non-stop flow of energy and/or momentum between the dark sectors are specified with these interactions. The expansion history of the universe may be influenced by this kind of energy flow at both the fundamental and perturbation levels. An interaction function, also known as the coupling function, is a crucial component of models involving the interacting dark energy. After specifying the interaction, the dynamics of the universe can be analyzed through either analytical and/or numerical methods. In the realm of field theory, a set of functions have been probed in literature [15–21]. The coupling function parameterization  $Q = 3H\xi f(DM, DE)$  [22] is used in a very common manner, where  $H$  is the universe’s Hubble parameter,  $f(DM, DE)$  is any continuous function of dark matter (DM), dark energy (DE) and  $\xi$  is the coupling parameter that describes the strength of interaction. In order to keep things simple, the coupling parameter is commonly regarded as time-independent. However, this fundamental notion has been challenged also [23–26]. Assuming a constant coupling parameter and a consistent equation of state for the dark energy, the components of coupling term only offers a basic comprehension of interactions within the dark sector of the universe. When the dark

energy equation of state fluctuates, it is crucial to consider the choice between a constant and dynamic coupling value and evaluate the fit quality of various interacting scenarios in light of observational constraints.

The idea of modified theories of gravity have gained popularity in the past few years as one of the finest clarifications to explain the current accelerated expansion of the universe. Modified gravity theory appears to be quite appealing in general, since it provides qualitative solutions to many key problems including dark energy. It is widely acknowledged that the general relativity in its fundamental state is unable to take responsibility for such phenomena during evolution of the universe without inclusion of either additional terms to the gravitational Lagrangian [27, 28] or the exotic fluid elements [29–31]. Numerous studies on modified gravity theories have proved its ability to replicate both the inflation and dark energy eras [32, 33]. The most fundamental modification of GTR is known as the  $f(R)$  gravity theories. In  $f(R)$  theory, the Hilbert-Einstein action is transformed by an arbitrary function of Ricci scalar  $R$  [34–37]. This concept may reconstruct not only the complete cosmic timeline but also the nature of the cosmological constant [38]. Furthermore, the performance of modified gravity appears promising at smaller scales, where a return to the GR limit is required, but all of these possibilities have their own flaws and before they can be approved as valid theories they have to pass extensive theoretical and observational testing [39]. For the well-defined modified gravity Lagrangian, the quasistatic approximation may yield peculiar results as compared to the  $\Lambda$  cold dark matter ( $\Lambda$ CDM) model [40]. The non-minimal theories of gravity may yield the stable de Sitter era of accelerating universe [41]. The non-minimal gravity theory termed as  $f(R, T)$  gravity may have the stable de Sitter and power-law solutions [42].

The  $f(R, \mathcal{G})$  gravity is a kind of theory that extends the ideas of  $f(R)$  and  $f(\mathcal{G})$  gravity. To better understand this, let us take a quick look at  $f(\mathcal{G})$  gravity. Similar to how  $f(R)$  gravity works, there is another idea in the world of modified gravity theories called Gauss-Bonnet (GB) gravity termed as  $f(\mathcal{G})$  gravity, where  $\mathcal{G} \equiv R - R_{\mu\nu}R^{\mu\nu} + R_{\mu\nu\alpha\beta}R^{\mu\nu\alpha\beta}$  is four dimensional topological invariant known as the Gauss-Bonnet term. In this gravity theory, the motion equation may team up with the scalar field and/or the  $f(\mathcal{G})$  may be an arbitrary function of  $\mathcal{G}$ . This theory could be useful in understanding the inflationary scenario when the universe expanded rapidly [43] as well as how the change from slowing down to speeding up happened. The Gauss-Bonnet gravity is found to have more degree of freedom compared to the  $f(R)$  gravity [44]. The  $f(\mathcal{G})$  gravity has been investigated for future singularities and acceleration of the universe in its later stages [45, 46]. Additionally, it offers explanations for cosmic acceleration followed by the era which is dominated by matter through some feasible models in  $f(\mathcal{G})$  gravity.

In this study, we investigate the  $f(R, \mathcal{G})$  gravity that transforms GTR action by the

functions of Ricci scalar ( $R$ ) and Gauss-Bonnet term ( $\mathcal{G}$ ). To address issues of the cosmic acceleration of universe, this framework provides an entirely new approach [47, 48]. The  $f(R, \mathcal{G})$  gravity offers the opportunity to go beyond conventional theories and gain a deeper understanding of the fundamental characteristics of the behavior of the universe. It accomplishes this by including both the curvature components and thus we can explore a theory in which both  $R$  and  $\mathcal{G}$  are incorporated in a non-linear way [49]. This theory allows us to fully utilize the range of curvature possibilities by extending GTR. The cosmic dynamics in modified gravity with the Gauss-Bonnet term and Ricci scalar term may have the dynamical evolution of General relativity in low-curvature limits [50]. The  $f(R, \mathcal{G})$  model may have cosmic evolution consistent with the observations [51]. The Einstein-Gauss-Bonnet theory with Gauss-Bonnet invariant and scalar field may have additional critical points and may explain the cosmic dynamics of the universe [52].

The main challenge with these kind of gravity theories is to get the analytical or numerical solutions, since the non-linear equations of motion makes it almost impossible to compare them to the observational data. Therefore, one may apply ‘alternative’ methods that can solve these equations effectively or at least be able to manage the general dynamical behavior of the universe. The dynamical system analysis is one of such technique. The objective of this analysis is to identify stability of critical points that may be used to explain the qualitative nature of universe evolution in model [53–55]. In a more fundamental way, the idea of the dynamical system constitutes the identification of critical points from the system of first-order differential equations and thus, the stability conditions can be extracted by computing the Jacobian matrix at critical points and searching out for their eigenvalues. The dynamical system analysis for different cosmological models in various theories of gravity are studied [41, 42, 49–66]. Interested readers may see comprehensive details on the utilization of dynamical systems analysis in cosmology [67–69].

The present study is sequentially structured into separate sections as follows: The Section 2 is focused on presenting the key equations of  $f(R, \mathcal{G})$  gravity framework, specifically addressing the action and field equations. In Section 3, we design a dynamical system, defining the relevant variables and write the equations describing their evolution. In the subsequent section 4, we analyze fixed points and their stability in the context of a specific  $f(R, \mathcal{G}) = \alpha R^m + \beta \mathcal{G}^n$  model. In section 5, we constrain the model parameters using observational Hubble and Pantheon data. In Section 6, we employ statefinder diagnostic technique to analyze the characteristics associated with critical points. We provide an overview of results from our investigation in Section 7.

## 2 The basic equations of $f(R, \mathcal{G})$ gravity framework

The action of  $f(R, \mathcal{G})$  gravity with canonical scalar field may be given by

$$S = \frac{1}{2\kappa^2} \int dx^4 \sqrt{-g} [f(R, \mathcal{G}) + \mathcal{L}_m + \mathcal{L}_\phi]. \quad (1)$$

Herein,  $f(R, \mathcal{G})$  represents a function involving both the Ricci scalar ( $R$ ), and the Gauss-Bonnet invariant ( $\mathcal{G}$ ). The standard matter Lagrangian density is denoted by  $\mathcal{L}_m$ . The Lagrangian of canonical scalar field  $\phi$  is denoted by  $\mathcal{L}_\phi \equiv \frac{1}{2}(\nabla\phi)^2 - V(\phi)$  where  $(\nabla\phi)^2 = g^{ij}\partial_i\partial_j\phi$ . And,  $\kappa^2 = 8\pi G$ , where  $G$  is the Newtonian gravitational constant and we standardise the units by setting  $c = k_B = \hbar = 1$ . The Gauss-Bonnet invariant may be described as follows:

$$\mathcal{G} \equiv R^2 - 4R_{ij}R^{ij} + R_{ijkl}R^{ijkl}. \quad (2)$$

The Einstein's field equations corresponding to the action (1) may be written by varying it with respect to the metric tensor field  $g_{ij}$  as

$$R_{ij} - \frac{1}{2}g_{ij}R = \kappa^2 T_{ij}^{(m)} + T_{ij}^{(GB)} + T_{ij}^{(\phi)}, \quad (3)$$

Here  $T_{ij}^{(m)}$ ,  $T_{ij}^{(GB)}$  and  $T_{ij}^{(\phi)}$  are the stress energy tensor for the matter, Gauss-Bonnet term and scalar field component, respectively. The stress-energy tensor for the standard matter is given by

$$T_{ij}^{(m)} = -\frac{2}{\sqrt{-g}} \frac{\delta(\sqrt{-g}\mathcal{L}_m)}{\delta g_{ij}}. \quad (4)$$

and the energy-momentum term corresponding to  $f(R, \mathcal{G})$  gravity as

$$\begin{aligned} T_{ij}^{(GB)} &= \nabla_i \nabla_j f_R - g_{ij} \square f_R + 2R \nabla_i \nabla_j f_{\mathcal{G}} - 2g_{ij} R \square f_{\mathcal{G}} - 4R_i^\lambda \nabla_\lambda \nabla_j f_{\mathcal{G}} - 4R_j^\lambda \nabla_\lambda \nabla_i f_{\mathcal{G}} \\ &+ 4R_{ij} \square f_{\mathcal{G}} + 4g_{ij} R^{kl} \nabla_k \nabla_l f_{\mathcal{G}} + 4R_{ijkl} \nabla^k \nabla^l f_{\mathcal{G}} - \frac{1}{2}g_{ij} (R f_R + \mathcal{G} f_{\mathcal{G}} - f) \\ &+ (1 - f_R) \left( R_{ij} - \frac{1}{2}g_{ij} R \right). \end{aligned} \quad (5)$$

where  $\square$  denotes the d'Alembert operator in the context of curved spacetime and we use

$$f_R \equiv \frac{\partial f(R, \mathcal{G})}{\partial R} \quad \text{and} \quad f_{\mathcal{G}} \equiv \frac{\partial f(R, \mathcal{G})}{\partial \mathcal{G}} \quad (6)$$

for the partial derivatives with respect to  $R$  and  $\mathcal{G}$ . The present analysis involves the FLRW metric applied to a spatially flat universe ( $k = 0$ ), featuring a scale factor  $a(t)$  that evolves over time. The metric is given by

$$ds^2 = -dt^2 + a^2(t)[dx^2 + dy^2 + dz^2] \quad (7)$$

In this case, the Ricci scalar and the Gauss-Bonnet invariant are given by

$$R = 6(2H^2 + \dot{H}), \quad (8)$$

$$\mathcal{G} = 24H^2(H^2 + \dot{H}), \quad (9)$$

The Hubble parameter, expressed as  $H = \dot{a}/a$ , where an overhead dot denotes the derivative with respect to cosmic time. Moreover, the field equations from equation (3) for the FLRW metric (7) would take the form

$$3f_R H^2 = \kappa^2(\rho_m + \rho_\phi) + \frac{1}{2}(f_R R - f - 6H\dot{f}_R + \mathcal{G}f_G - 24H^3\dot{f}_G), \quad (10)$$

$$2f_R \dot{H} = -\kappa^2(p_m + p_\phi + \rho_m + \rho_\phi) + H\dot{f}_R - \ddot{f}_R + 4H^3\dot{f}_G - 8H\dot{H}f_G - 4H^2\ddot{f}_G \quad (11)$$

The equations (10) and (11) can be rewritten by applying new definitions as

$$3f_R H^2 = \kappa^2(\rho_m + \rho_\phi + \rho_\Lambda) \quad (12)$$

$$2f_R \dot{H} = -\kappa^2(\rho_m + p_m + p_\phi + \rho_\phi + \rho_\Lambda + p_\Lambda). \quad (13)$$

The energy density ( $\rho_\phi$ ) and pressure ( $p_\phi$ ) for the canonical scalar field may be given by

$$\rho_\phi = \frac{1}{2}\dot{\phi}^2 + V(\phi) \quad (14)$$

$$p_\phi = \frac{1}{2}\dot{\phi}^2 - V(\phi). \quad (15)$$

Here, we are looking into quintessence field with an exponential potential [57], which is given by

$$V(\phi) = V_0 e^{-\lambda\phi} \quad (16)$$

including a dimensionless parameter  $\lambda$ , with the condition,  $V_0 > 0$ . Using Equations (14) and (15), the equation given above may be expressed as

$$3f_R H^2 = \kappa^2(\rho_m + \frac{1}{2}\dot{\phi}^2 + V(\phi) + \rho_\Lambda) \quad (17)$$

$$2f_R \dot{H} = -\kappa^2(\rho_m + \dot{\phi}^2 + \rho_\Lambda + p_\Lambda) \quad (18)$$

From equations (10), (11), (17) and (18), we have

$$\kappa^2 \rho_\Lambda = \frac{1}{2}(f_R R - f - 6H\dot{f}_R + \mathcal{G}f_G - 24H^3\dot{f}_G) \quad (19)$$

$$-\kappa^2(\rho_\Lambda + p_\Lambda) = H\dot{f}_R - \ddot{f}_R + 4H^3\dot{f}_G - 8H\dot{H}f_G - 4H^2\ddot{f}_G \quad (20)$$

In this way, the energy density  $\rho_\Lambda$  and pressure  $p_\Lambda$  of the geometrical dark energy may follow the conservation equation as

$$\dot{\rho}_\Lambda = -3H(\rho_\Lambda + p_\Lambda). \quad (21)$$

where the equation of state parameter  $\omega_\Lambda = \frac{p_\Lambda}{\rho_\Lambda}$  is defined by

$$\omega_\Lambda = \frac{p_\Lambda}{\rho_\Lambda} = -1 - \frac{H\dot{f}_R - \ddot{f}_R + 4H^3\dot{f}_G - 8H\dot{H}\dot{f}_G - 4H^2\ddot{f}_G}{\frac{1}{2}(f_R R - f - 6H\dot{f}_R + \mathcal{G}f_G - 24H^3\dot{f}_G)} \quad (22)$$

We assume the interaction between the matter energy  $\rho_m$  and scalar field  $\rho_\phi$ . This is done by introducing the parameter  $Q$  which plays an important role in controlling the energy exchange rate in the dark sector. The energy moves from dark matter to dark energy in situations where  $Q > 0$ ; in contrast, the energy moves from dark energy to dark matter in situations where  $Q < 0$ . The interaction between a quintessence scalar field  $\phi$  and dark matter, including its energy density  $\rho_m$ , can be comprehensively depicted through balance equations

$$\dot{\rho}_\phi = -3H(1 + \gamma_\phi)\rho_\phi + Q \quad (23)$$

$$\dot{\rho}_m = -3H\rho_m - Q. \quad (24)$$

where  $p_\phi = \gamma_\phi\rho_\phi$ . Using equation (14) and (15) in equation (23), we may write the propagation equation of scalar field  $\phi$  with the dark sector coupling parameter  $Q$  as [61, 70]

$$\ddot{\phi} + 3H\dot{\phi} + \frac{dV}{d\phi} = \frac{Q}{\dot{\phi}} \quad (25)$$

We define the effective equation of state parameter as

$$\omega_{eff} = -1 - \frac{2\dot{H}}{3H^2}. \quad (26)$$

In the effective scenario, we take the matter fluid (satisfying  $p_m = 0$ ) to be interacting with scalar field satisfying  $p_\phi = \gamma_\phi\rho_\phi$  in the  $f(R, G)$  gravity framework. This set-up yields us the degree of freedom and helps us to reduce the non-linearity associated with the traditional  $f(R, G)$  gravity field equations. It is worthwhile to mention that the  $f(R, G)$  models may not be always written in form of autonomous system with non-linear exponents of Gauss-Bonnet invariant [71]. By using equations (10) and (14), we may write as

$$1 = \frac{\kappa^2\rho_m}{3f_R H^2} + \frac{\kappa^2\dot{\phi}^2}{6f_R H^2} + \frac{\kappa^2 V(\phi)}{3f_R H^2} + \frac{R}{6H^2} - \frac{f}{6f_R H^2} - \frac{\dot{f}_R}{f_R H} + \frac{\mathcal{G}f_G}{6f_R H^2} - \frac{4H\dot{f}_G}{f_R}. \quad (27)$$

### 3 Dynamical systems analysis of the $f(R, G)$ model

In this section, we use the dynamical system technique to study the universe evolution in model. In the dynamical system formulation of the cosmological models, the cosmological

equations of model are converted into the autonomous system. In the autonomous system, the independent variable does not appear explicitly [56]. For the dynamical system given by  $\dot{x} = f(x)$ , where  $x = (x_1, x_2, x_3, \dots, x_n)$ , the critical points may be calculated by solving  $\dot{x} = 0$ . The Jacobian matrix evaluated at critical points will possess eigenvalues. The eigenvalues are used to conclude on the stability of critical points of the cosmological dynamical system. If all the eigenvalues are of positive sign, then the critical point may be termed as unstable point. This kind of point is also termed as source or repeller of the system. In the phase space, the trajectories seem to diverge from the unstable point. If all the eigenvalues are of negative sign, then the critical point may be termed as the stable point. This kind of point is also known as the sink or attractor of the system. In the phase space, the trajectories seem to converge at the stable point. The points having eigenvalues of mixed signs are known as the saddle points. In the case of saddle points, the trajectories in the phase space would be converging along directions of negative signs and diverging along the directions having positive signs of eigenvalues [67, 68]. The dynamical system of cosmological model may exhibit the cosmological phases of universe evolution corresponding to critical points. The attractor of cosmological dynamical system reveals about the accelerating universe expansion of late-time era. The saddle points are suitable to portray the intermediate era of universe expansion such as the matter dominated era. The unstable critical points are suitable to portray the beginning era of the universe in a cosmological dynamical system [69]. We use these criterion to study the  $f(R, G)$  model using dynamical system. In order to study the  $f(R, G)$  model using the dynamical system analysis, we define the dimensionless variables as

$$\begin{aligned} x_1 &= \frac{\kappa^2 \rho_m}{3f_R H^2}, & x_2 &= \frac{\kappa^2 \dot{\phi}^2}{6f_R H^2}, & x_3 &= \frac{\kappa^2 V(\phi)}{3f_R H^2}, & x_4 &= \frac{R}{6H^2}, & x_5 &= \frac{f}{6f_R H^2}, \\ x_6 &= \frac{\dot{f}_R}{f_R H}, & x_7 &= \frac{\mathcal{G} \dot{f}_G}{6f_R H^2}, & x_8 &= \frac{4H \dot{f}_G}{f_R}. \end{aligned} \quad (28)$$

Using equation (28), the equation (27) may be written as

$$1 = x_1 + x_2 + x_3 + x_4 - x_5 - x_6 + x_7 - x_8 \quad (29)$$

along with the density parameters

$$x_1 = \Omega_m, \quad x_2 + x_3 = \Omega_\phi, \quad x_4 - x_5 - x_6 + x_7 - x_8 = \Omega_\Lambda. \quad (30)$$

We use a dimensionless time variable  $N = |\ln a(t)|$  in our model. The formulation of the following dynamical system is achieved by computing the derivative of these variables



with respect to  $N$ . The dynamical system of the present framework may be written as

$$\frac{dx_1}{dN} = -6x_1 - x_1x_6 - 2x_1\frac{\dot{H}}{H^2} \quad (31)$$

$$\frac{dx_2}{dN} = 3\xi x_1 - 6x_2 + \lambda\frac{\dot{\phi}}{H}x_3 - x_2x_6 - 2x_2\frac{\dot{H}}{H^2} \quad (32)$$

$$\frac{dx_3}{dN} = -\lambda\frac{\dot{\phi}}{H}x_3 - x_3x_6 - 2x_3\frac{\dot{H}}{H^2} \quad (33)$$

$$\frac{dx_4}{dN} = \frac{\dot{R}}{6H^3} - 2x_4\frac{\dot{H}}{H^2} \quad (34)$$

$$\frac{dx_5}{dN} = \frac{\dot{f}}{6f_R H^3} - x_5x_6 - 2x_5\frac{\dot{H}}{H^2} \quad (35)$$

$$\frac{dx_6}{dN} = \frac{\ddot{f}_R}{f_R H^2} - x_6^2 - x_6\frac{\dot{H}}{H^2} \quad (36)$$

$$\frac{dx_7}{dN} = \frac{\dot{\mathcal{G}}}{\mathcal{G}H}x_7 + \frac{\mathcal{G}}{24H^4}x_8 - x_6x_7 - 2x_7\frac{\dot{H}}{H^2} \quad (37)$$

$$\frac{dx_8}{dN} = x_8\frac{\dot{H}}{H^2} + \frac{4\ddot{f}_\mathcal{G}}{f_R} - x_6x_8 \quad (38)$$

For the system to be closed, it is essential that all terms on the right-hand side of the mentioned equations are represented in terms of the variables indicated in equation (28). Here, we consider  $Q = 3H\xi\rho_m$ . From equations (8), (9), and (11), we determine the necessary expressions as

$$\frac{\dot{H}}{H^2} = x_4 - 2 \quad (39)$$

$$\frac{\dot{f}}{6f_R H^3} = \frac{x_4x_6}{b} + \frac{x_7}{x_4 - 1} \left[ \frac{x_4x_6}{b} + 2(x_4 - 2)^2 \right] \quad (40)$$

$$\frac{\dot{R}}{6H^3} = \frac{x_4x_6}{b} \quad (41)$$

$$\frac{\dot{\mathcal{G}}}{\mathcal{G}H} = \frac{1}{(x_4 - 1)} \left[ \frac{x_4x_6}{b} + 2(x_4 - 2)^2 \right] \quad (42)$$

$$\frac{\mathcal{G}}{24H^4} = x_4 - 1 \quad (43)$$

$$\frac{4\ddot{f}_\mathcal{G}}{f_R} = -6x_2 - 3x_1 + x_6 + x_8(5 - 2x_4) - 2(x_4 - 2) - \frac{\ddot{f}_R}{f_R H^2}. \quad (44)$$

Using equations (39-44), the system (31-38) may be transformed as

$$\frac{dx_1}{dN} = -6x_1 - x_1x_6 - 2x_1(x_4 - 2) \quad (45)$$

$$\frac{dx_2}{dN} = 3\xi x_1 - 6x_2 + \lambda \frac{\dot{\phi}}{H} x_3 - x_2x_6 - 2x_2(x_4 - 2) \quad (46)$$

$$\frac{dx_3}{dN} = -\lambda \frac{\dot{\phi}}{H} x_3 - x_3x_6 - 2x_3(x_4 - 2) \quad (47)$$

$$\frac{dx_4}{dN} = \frac{x_4x_6}{b} - 2x_4(x_4 - 2) \quad (48)$$

$$\frac{dx_5}{dN} = \frac{x_4x_6}{b} + \frac{x_7}{x_4 - 1} \left[ \frac{x_4x_6}{b} + 2(x_4 - 2)^2 \right] - x_5x_6 - 2x_5(x_4 - 2) \quad (49)$$

$$\frac{dx_6}{dN} = \Gamma - x_6^2 - x_6(x_4 - 2) \quad (50)$$

$$\frac{dx_7}{dN} = \frac{x_7}{x_4 - 1} \left[ \frac{x_4x_6}{b} + 2(x_4 - 2)^2 \right] + (x_4 - 1)x_8 - x_7x_6 - 2x_7(x_4 - 2) \quad (51)$$

$$\frac{dx_8}{dN} = -x_8(x_4 + x_6 - 3) - 3x_1 - 6x_2 + x_6 - 2(x_4 - 2) - \Gamma \quad (52)$$

where

$$b = \frac{d \ln f_R}{d \ln R} = \frac{R f_{RR}}{f_R} \quad (53)$$

These equations would govern the cosmological evolution within a generalized  $f(R, \mathcal{G})$  gravity theory, with the specific nature of the theory describe by  $\Gamma = \frac{\ddot{f}_R}{f_R H^2}$ . Furthermore, we also have

$$\omega_{eff} = -\frac{1}{3}(2x_4 - 1) \quad (54)$$

$$\omega_\Lambda = -1 - \frac{3x_1 + 6x_2 + 2x_4 - 4}{3(1 - x_1 - x_2 - x_3)}. \quad (55)$$

Additionally, the deceleration parameter is obtained as

$$q = \frac{d}{dt} \left( \frac{1}{H} \right) - 1 = -1 - \frac{\dot{H}}{H^2} = 1 - x_4 \quad (56)$$

As a general rule, the system is considered open until the expression for  $\Gamma$  is presented in terms of the dynamical variables (28). A particular case of  $f(R, \mathcal{G})$  may be considered and its dynamics and stability in a flat FLRW universe may be examined. The  $f(R, \mathcal{G})$  functional forms such as  $f(R, \mathcal{G}) \equiv \alpha R^m + \beta \mathcal{G}^n$  and  $f(R, \mathcal{G}) \equiv f_0 R^\delta \mathcal{G}^\mu$  are allowed by the Noether symmetry method [72]. The dynamical system and observational analysis of model having  $f(R, \mathcal{G}) \equiv f_0 R^\delta \mathcal{G}^\mu$  form have been well-explored [49, 51, 71, 72]. We probe the dynamical evolution in  $f(R, \mathcal{G}) \equiv \alpha R^m + \beta \mathcal{G}^n$  model whose form is admitted in Noether symmetry analysis.

In other words, we proceed with the choice of  $f(R, \mathcal{G}) \equiv \alpha R^m + \beta \mathcal{G}^n$  characterized by parameters  $\alpha, \beta, m$ , and  $n$  gravity and we choose the coupling parameter  $Q = 3H\xi\rho_m$  in our calculations. This model stands as a generalization of different gravity theories. Specifically, setting  $\alpha \neq 0, \beta = 0$ , and  $m = 1$  yields Einstein's gravity, while  $\alpha \neq 0, \beta = 0$ , and  $m = 2$  corresponds to  $R^2$  gravity, and  $\alpha \neq 0, \beta = 0$  results in  $f(R)$ . Furthermore, in the case of  $\alpha = 0, \beta \neq 0$ , the model transforms into  $f(\mathcal{G})$  gravity. Moreover, we consider  $\phi = \ln H^{m_1}$  where  $H$  is Hubble parameter and  $m_1$  is arbitrary positive real number. Consequently, the relation  $\frac{\lambda\dot{\phi}}{H} = K(x_4 - 2)$  may be obtained, where  $K = \lambda.m_1$  serves as a constant with  $\lambda > 0$  and  $m_1 > 0$ . The combination of equations (28) and (53) contributes to different relations between dynamical variables. Specifically, we may have

$$b = (m - 1), \quad (57)$$

$$x_5 = \frac{x_4}{m} + \frac{x_7}{n}, \quad (58)$$

$$x_8 = \frac{(n-1)x_7}{(x_4-1)^2} \left[ \frac{x_4 x_6}{b} + 2(x_4 - 2)^2 \right] \quad (59)$$

$$x_6 = \frac{-1 + x_1 + x_2 + x_3 + x_4 \left( \frac{m-1}{m} \right) + \frac{x_7(n-1)}{(x_4-1)^2} \left[ \frac{(x_4-1)^2}{n} - 2(x_4-2)^2 \right]}{1 + \frac{(n-1)x_4 x_7}{b(x_4-1)^2}}. \quad (60)$$

By using above equations (57-60), we may thus rule out  $x_5, x_6$ , and  $x_8$ , since these variables are depending on other variables. From Eqs. (45-52), the autonomous system of the model would take the form

$$\frac{dx_1}{dN} = -6x_1 - x_1 x_6 - 2x_1(x_4 - 2) \quad (61)$$

$$\frac{dx_2}{dN} = 3\xi x_1 - 6x_2 + K(x_4 - 2)x_3 - x_2 x_6 - 2x_2(x_4 - 2) \quad (62)$$

$$\frac{dx_3}{dN} = -K(x_4 - 2)x_3 - x_3 x_6 - 2x_3(x_4 - 2) \quad (63)$$

$$\frac{dx_4}{dN} = \frac{x_4 x_6}{m-1} - 2x_4(x_4 - 2) \quad (64)$$

$$\frac{dx_7}{dN} = \frac{x_7}{x_4 - 1} \left[ \frac{x_4 x_6}{b} + 2(x_4 - 2)^2 \right] + (x_4 - 1)x_8 - x_7 x_6 - 2x_7(x_4 - 2) \quad (65)$$

We may obtain the critical points of the above system and determine their stability.

## 4 The critical points and their cosmological implications

For getting the fixed points, we equate the autonomous system (61-65) to zero. The fixed points coordinates  $(x_1, x_2, x_3, x_4, x_7)$  and the corresponding EoS parameter  $(\omega_{eff})$

are given in Table 1. The summary of eigenvalues at the critical points are given in Table 2.

| Critical points | $(x_1, x_2, x_3, x_4, x_7)$                            | $\omega_{eff}$  |
|-----------------|--|---|
| A               | $(0, 0, 0, 0, 0)$                                      | $\frac{1}{3}$   |
| B               | $(0, -1, 0, 0, 0)$                                     | $\frac{1}{3}$   |
| C               | $(0, 0, 0, 0, \frac{8n^2-5n}{(8n-1)(n-1)})$            | $\frac{1}{3}$   |
| D               | $(0, \frac{-K(2K+5)}{3}, \frac{(2K+5)(K+3)}{3}, 0, 0)$ | $\frac{1}{3}$   |
| E               | $(0, \frac{-(7m^2-11m+3)}{m^2}, 0, \frac{2m-3}{m}, 0)$ | $\frac{2m-3}{m}$  |
| F               | $(0, 0, 0, 2, \frac{-(2n-mn)}{m-mn})$                  | $-1$  |
| G               | $(0, 0, 0, \frac{4m^2-5m}{(2m-1)(m-1)}, 0)$            | $-\frac{1}{3} \frac{(-6m^2 + 7m + 1)}{(2m^2 - 3m + 1)}$ |

Table 1: The critical points and their corresponding effective equation of state parameter

| Critical points | Eigenvalues  |
|-----------------|--|
| A               | $[-1, -1, 2K + 5, 5 - 8n, \frac{4m-5}{m-1}]$                                 |
| B               | $[0, 1, 2K + 6, 6 - 8n, \frac{4m-6}{m-1}]$                                   |
| C               | $[8n - 5, 8n - 6, 8n - 6, \frac{4m-8n}{m-1}, 2K + 8n]$                       |
| D               | $[-2K - 5, -2K - 6, -2K - 6, \frac{2K+4m}{m-1}, -2K - 8n]$                   |
| E               | $[0, \frac{3K+6m}{m}, \frac{6m-12n}{m}, \lambda_{4E}, \lambda_{5E}]$         |
| F               | $[-6, -6, 0, \lambda_{4F}, \lambda_{5F}]$                                    |
| G               | $[\lambda_{1G}, \lambda_{2G}, \lambda_{3G}, \lambda_{4G}, \frac{5-4m}{m-1}]$ |

Table 2: The eigenvalues corresponding to the critical points, where  $\lambda_{4E} = \frac{(121m^3-371m^2+339m-81)^{1/2}-3(m-1)^{3/2}}{2m(m-1)^{1/2}}$ ,  $\lambda_{5E} = \frac{(121m^3-371m^2+339m-81)^{1/2}+3(m-1)^{3/2}}{2m(m-1)^{1/2}}$ ,  $\lambda_{4F} = \frac{-1}{2}(\frac{41m-100n+50mn-25n^2}{m-4n+2mn-m^2})^{1/2} - \frac{3}{2}$ ,  $\lambda_{5F} = \frac{1}{2}(\frac{41m-100n+50mn-25n^2}{m-4n+2mn-m^2})^{1/2} - \frac{3}{2}$ ,  $\lambda_{1G} = \frac{(2K+4m-Km-2m^2)}{2m^2-3m+1}$ ,  $\lambda_{2G} = \frac{(4m-8n+4mn-2m^2)}{2m^2-3m+1}$ ,  $\lambda_{3G} = \frac{-(14m^2-22m+6)}{2m^2-3m+1} = \lambda_{4G}$ .

The eigenvalues of the system (61-65) may be used to examine the stability of critical

points. This system (61-65) has seven critical points. The stability nature and cosmological properties at the critical points are summarized as follows:

*Point A:* This point will always be in existence, irrespective of the model parameters values. This point acts like a saddle point for all values of  $m$  and  $n$  with the exceptions  $m \neq 1, 5/4$  and  $n \neq 5/8$ .

Associated with this point, the deceleration parameter and the effective EoS parameter are given by  $q = 1$  and  $\omega_{eff} = 1/3$  respectively. This is the point where the cosmos is in a state of decelerated expansion dominated by effective radiation-like fluid with the Hubble parameter,  $H = \frac{C_1}{1 + 2C_1t}$ . Moreover, the scale factor is given by integrating the relation  $H = \frac{\dot{a}}{a}$  as  $a \propto (1 + 2C_1t)^{1/2}$ , where  $C_1$  is an integration constant. Additionally, the effective EoS parameter suggests that the universe is primarily governed by radiation.

*Point B:* The point B(0, -1, 0, 0, 0) will always exist. The behavior of this point is like a repeller for  $m < 1$  or  $m > 3/2$  and  $n < 3/4$  and; for  $m \in (1, 3/2)$  and  $n > 3/4$  it behaves like a saddle point. Connected to this point, the values of deceleration parameter  $q$  and the effective equation of state parameter  $\omega_{eff}$  are 1 and 1/3 respectively. This marks the era when the universe expansion is slowing down and is dominated by radiation. Moreover, in this case, the Hubble parameter and the scale factor respective values are given by  $H = \frac{C_2}{1 + 2C_2t}$  and  $a \propto (1 + 2C_2t)^{1/2}$ , where  $C_2$  is an integration constant.

*Point C:* The presence of the critical point C(0, 0, 0, 0,  $\frac{8n^2-5n}{(8n-1)(n-1)}$ ) in the cosmological system persists as long as the condition  $n \neq 1/8, 1$  is satisfied. For the cases  $m > 3/2$ , the point behaves like a repeller. The cases where  $n \in (0, 5/8) \cup (5/8, 3/4)$  and  $m \neq 2n$ , the point will acts like a saddle point. For  $m < 2n$  or  $m > 1$  and  $n < -K/4 < 0$ , this point will remain stable. The corresponding deceleration parameter  $q$  and the effective EoS parameter  $\omega_{eff}$  will have values 1 and 1/3 respectively. This is the point at which the expansion of the cosmos is slowing down under the influence of radiation-like effective fluid. Furthermore, in this scenario, the values of the Hubble parameter and the scale factor are respectively given by  $H = \frac{C_3}{1 + 2C_3t}$  and  $a \propto (1 + 2C_3t)^{1/2}$ , where  $C_3$  is an integration constant.

*Point D:* The critical point D(0,  $\frac{-K(2K+5)}{3}$ ,  $\frac{(2K+5)(K+3)}{3}$ , 0, 0) will continuously present in the cosmological dynamical system of model. This point will demonstrate stability, when the conditions  $m < -K/2 < 0$ , or  $m > 1, n > -K/4$ . and  $m > -K/2$ , or  $m < 1, n > -K/4$  are satisfied. Moreover, when the conditions  $m > -K/2, m > 1, n < -K/4 < 0$  and  $m < -K/2 < 0, m < 1, n < -K/4 < 0$  are fulfilled, then this point will exhibit saddle behavior. In connection with this, the effective EoS parameter  $\omega_{eff}$  and the deceleration parameter  $q$  will have values 1/3 and 1, respectively. In the era governed by this point, radiation will be taking over and the universe's expansion will be slowing

down. Moreover, in this case, the Hubble parameter and the scale factor are respectively given by  $H = \frac{C_4}{1 + 2C_4t}$  and  $a \propto (1 + 2C_4t)^{1/2}$ , where  $C_4$  is an integration constant.

*Point E:* The critical point E  $\left(0, \frac{-(7m^2-11m+3)}{m^2}, 0, \frac{2m-3}{m}, 0\right)$  will exist whenever  $m \neq 0$ . This point shows saddle behavior for  $m > 1$  and  $n < m/2$ . In this case, the expansion of the universe is marked by the the Hubble parameter,  $H = \frac{m}{mC_5 + 3t}$  and the scale factor will follow  $a \propto (mC_5 + 3t)^{m/3}$ , where  $C_5$  is an integration constant. The deceleration parameter is given by  $\frac{3}{m} - 1$ . Therefore, if the value of  $m$  satisfies the range  $m < 3$ , the cosmos will experience a decelerating phase of expansion and for  $m > 3$ , the universe will undergo an accelerating phase of expansion. In this scenario, the effective equation of state  $\omega_{eff}$  will be given by  $\frac{m-2}{m}$ . Consequently, the universe will be categorized as matter and radiation dominated for  $m = 2$  and  $m = 3$  respectively. For  $m = 1$  the value of  $\omega_{eff}$  will be  $-1$  which signifies the presence of the cosmological constant. In this particular scenario, the universe is dominated by a variant of energy known as the vacuum energy.

*Point F:* Under the constraint  $n \neq 1, m \neq 0$ , the critical point F  $\left(0, 0, 0, 2, \frac{-(2n-mn)}{m-mn}\right)$  continues to exist in the cosmological dynamical system. The point exhibits saddle behavior when the condition  $n > \frac{m(m-1)}{2(m-2)}$  holds. In this particular case, the expansion of the universe is identified by the Hubble parameter  $H = \frac{1}{C_6}$  and the scale factor  $a \propto \exp\left(\frac{t}{C_6}\right)$ , where  $C_6$  is an integration constant. Moreover, the value of the deceleration parameter  $q$  is given by  $-1$  which represents the de Sitter universe having exponential expansion. Consequently, the effective EoS parameter  $\omega_{eff} = -1$ . This represents a specific situation acknowledged as the cosmological constant or vacuum energy scenario.

*Point G:* Under the constraint  $m \neq 1, 1/2$ , the critical point G  $\left(0, 0, 0, \frac{4m^2-5m}{(2m-1)(m-1)}, 0\right)$  will exist in the cosmological dynamical system. It is noticed that point G exhibits an unstable nature for  $m < -K/2 < 0, m \in \left(\frac{11-\sqrt{37}}{14}, \frac{1}{2}\right) \cup \left(1, \frac{11+\sqrt{37}}{14}\right) \cup \left(1, \frac{5}{4}\right)$  and  $n < m/2$ . For  $-K/2 < m < 0, m \in \left(-\infty, \frac{11-\sqrt{37}}{14}\right) \cup \left(\frac{1}{2}, 1\right) \cup \left(\frac{11+\sqrt{37}}{14}, \infty\right) \cup (-\infty, 1) \cup \left(\frac{5}{4}, \infty\right)$  and  $n > m/2$ , it will act like an attractor otherwise, it will show saddle behavior. The expansion of the universe is identified through the Hubble parameter  $H = \frac{1}{Mt + C_7}$  and the scale factor is governed by the expression  $a \propto (Mt + C_7)^{1/M}$ , where  $M = \frac{2-m}{2m^2-3m+1}$ , and  $C_7$  is an integration constant.

In addition to this, the value of the deceleration parameter is expressed as  $q = \frac{-2m^2+2m+1}{2m^2-3m+1}$ . Therefore, the universe will undergo the accelerating expansion for  $m = 2$  and decelerating for  $m = 0$  or  $m = 5/4$ . The effective equation of state parameter will be  $\omega_{eff} = \frac{6m^2-7m-1}{3(2m^2-3m+1)}$ . If the value of  $m$  falls within the range  $m \in \left(\frac{4-\sqrt{10}}{6}, \frac{4+\sqrt{10}}{6}\right)$ , the

point will be governed by quintessence kind of dark energy and, for  $m \in \left(-\infty, \frac{4 - \sqrt{10}}{6}\right) \cup \left(\frac{4 + \sqrt{10}}{6}, \infty\right)$ , it will have the phantom kind of dark energy. Additionally, the universe will be classified as the matter and radiation dominated for  $m = \frac{7 \pm \sqrt{73}}{12}$  and  $m = \frac{1 \pm \sqrt{3}}{2}$  respectively. The value of  $\omega_{eff} = -1$  will lead to  $m = \frac{4 \pm \sqrt{10}}{6}$ . In Figures (1-7), we plot the 3-dimensional projections of the 5-dimensional autonomous system (61-65).

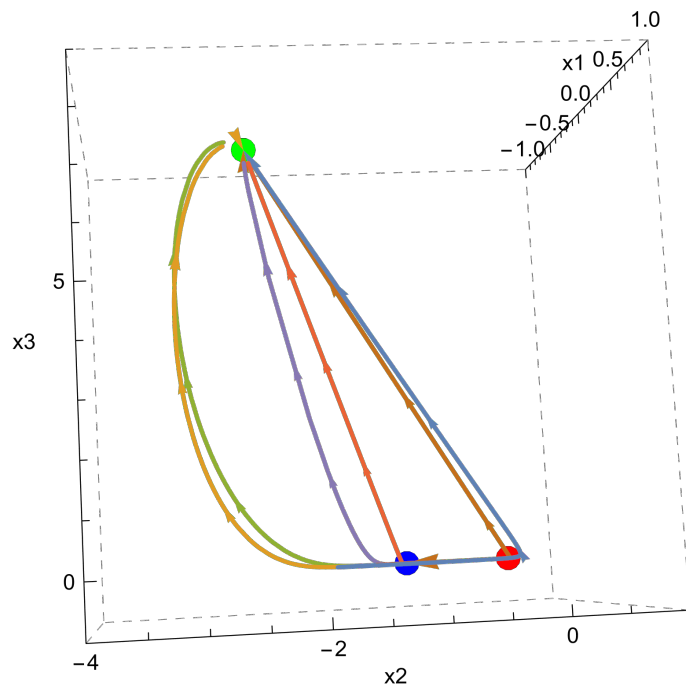


Figure 1: 3D Phase portrait in  $x_1 - x_2 - x_3$  plane for  $K = 1$  with coordinates of red point  $(0, 0, 0)$ , blue point  $(0, -1, 0)$ , and green point  $(0, -\frac{12}{5}, \frac{42}{5})$ .

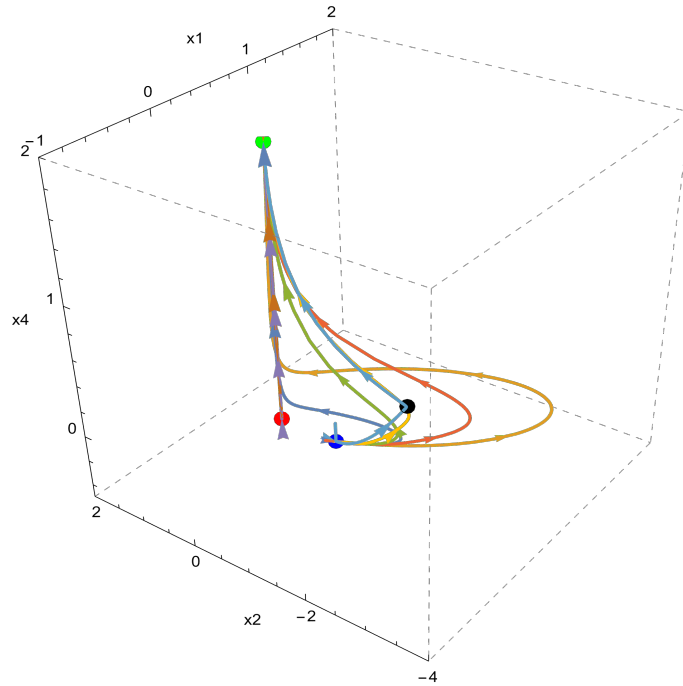


Figure 2: 3D Phase portrait in  $x_1 - x_2 - x_4$  plane for  $m = 2$  with coordinates of red point  $(0, 0, 0)$ , blue point  $(0, -1, 0)$ , green point  $(0, 0, 2)$ , and black point  $(0, -\frac{9}{4}, \frac{1}{2})$ .

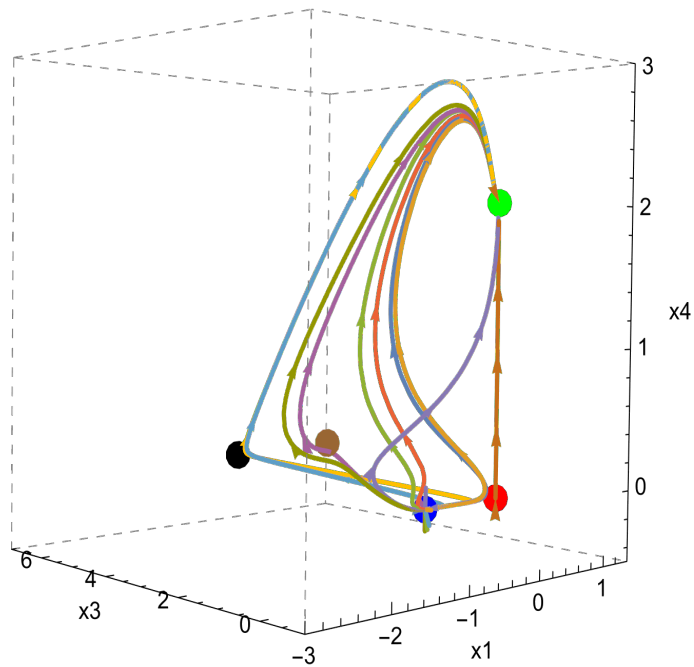


Figure 3: 3D Phase portrait in  $x_1 - x_3 - x_4$  plane for  $m = 2, K = 1$  with coordinates of red point  $(0, 0, 0)$ , blue point  $(-1, 0, 0)$ , green point  $(0, 0, 2)$ , black point  $(0, 7, 0)$ , and brown point  $(0, -\frac{9}{4}, \frac{1}{2})$ .



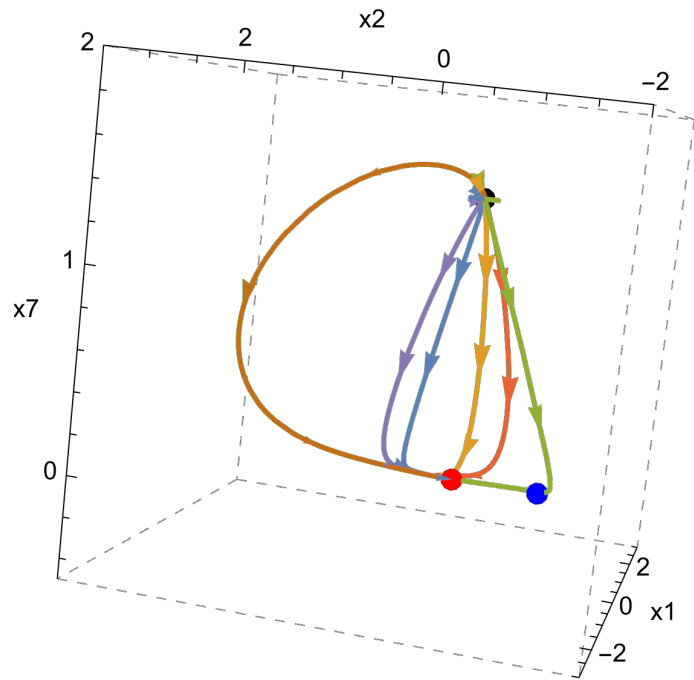


Figure 4: 3D Phase portrait in  $x_1 - x_2 - x_7$  plane for  $n = 2$  with coordinates of red point  $(0, 0, 0)$ , blue point  $(0, -1, 0)$ , and black point  $(0, 0, \frac{22}{15})$

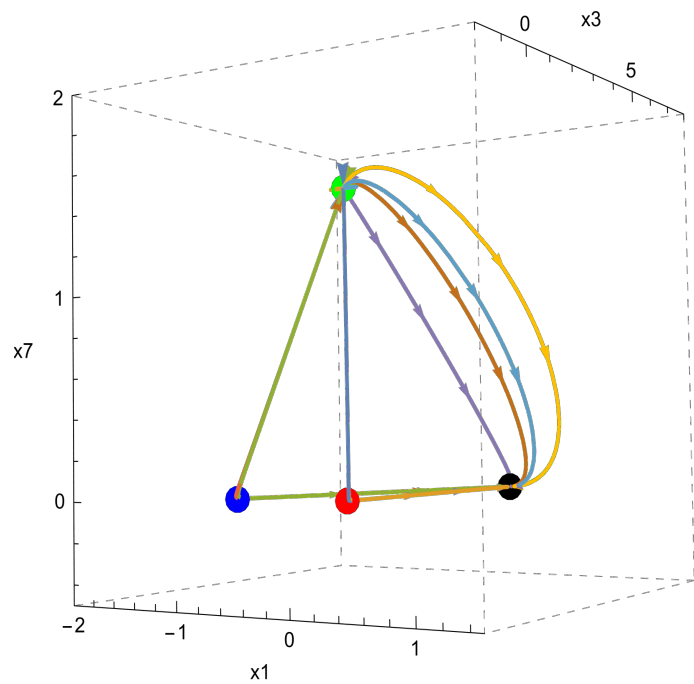


Figure 5: 3D Phase portrait in  $x_1 - x_3 - x_7$  plane for  $n = 2, K = 1$  with coordinates of red point  $(0, 0, 0)$ , blue point  $(-1, 0, 0)$ , green point  $(0, 0, \frac{22}{15})$ , and black point  $(0, 7, 0)$

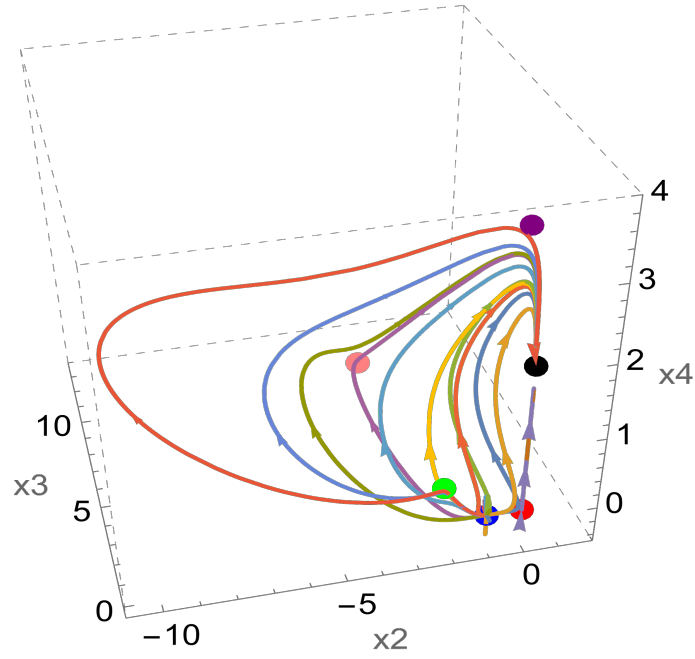


Figure 6: 3D Phase portrait in  $x_2 - x_3 - x_4$  plane for  $m = 2, K = 1$  with coordinates of red point  $(0, 0, 0)$ , blue point  $(-1, 0, 0)$ , green point  $(-\frac{9}{4}, 0, \frac{1}{2})$ , black point  $(0, 0, 2)$ , pink point  $(-\frac{7}{3}, -\frac{28}{3}, 0)$  and purple point  $(\frac{4}{19}, -\frac{34}{19}, \frac{10}{3})$

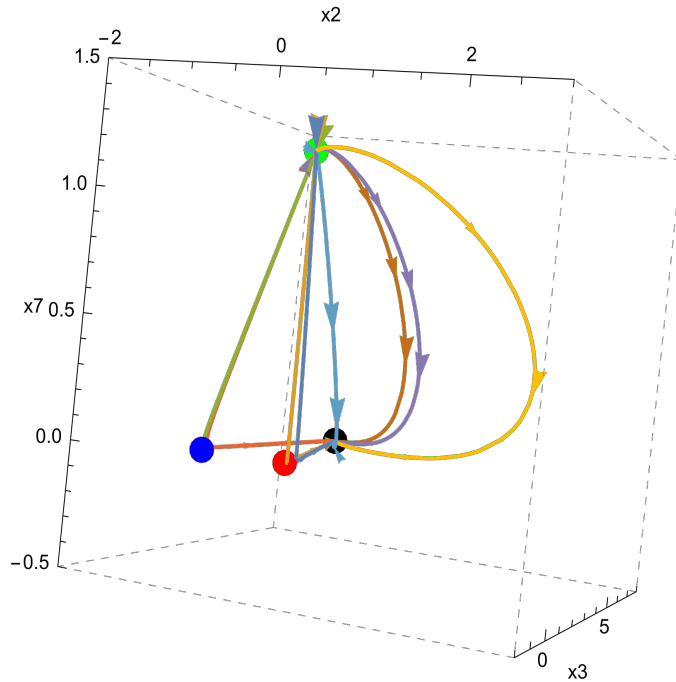


Figure 7: 3D Phase portrait in  $x_2 - x_3 - x_7$  plane for  $n = 3, K = 1/2$  with coordinates of red point  $(0, 0, 0)$ , blue point  $(-1, 0, 0)$ , green point  $(0, 0, \frac{57}{46})$ , and black point  $(-1, 7, 0)$

## 5 Constraint from the observational Hubble data and Pantheon data

In this section, we use the cosmological solutions corresponding to the dynamical system. The critical point of the cosmological dynamical system corresponds to the cosmic phase of the universe evolution in model. The  $f(R, \mathcal{G})$  model with interacting dark matter and scalar field possess different phases corresponding to points  $E$ ,  $F$ ,  $G$  and either of  $A$  or  $B/C/D$ . The effective fluid corresponding to point  $A/B/C/D$  follows  $\omega_{eff} = \frac{1}{3}$ . In this effective phase,  $\rho_r = \rho_{r0}a^{-4}$  which is primarily yielded by dynamical variables related to  $f(R, \mathcal{G})$  function. The effective fluid corresponding to point  $F$  will follow  $\rho_\Lambda = \rho_{\Lambda 0}$ . And, the effective fluid corresponding to point  $G$  will follow  $\rho_{m1} = \rho_{m10}a^{-\frac{-2(6m^2-8m+1)}{(2m-1)(m-1)}}$ . For the point  $E$ , the effective fluid will have  $\rho_{m2} = \rho_{m20}a^{-9(1-\frac{1}{m})}$ . These deductions are motivated with the fact that the effective EoS parameter during any cosmological phase may be related to the effective conservation equation ( $\dot{\rho} + 3H(1 + \omega_{eff}) = 0$ ) in that phase. Using this analogy, we write the effective Hubble parameter of the model as

$$H^2 = H_0^2 \left[ \Omega_r a^{-4} + \Omega_\Lambda + \Omega_{m1} a^{-\frac{-2(6m^2-8m+1)}{(2m-1)(m-1)}} + \Omega_{m2} a^{-9(1-\frac{1}{m})} \right] \quad (66)$$

where  $\Omega_r$ ,  $\Omega_\Lambda$ ,  $\Omega_{m1}$ , and  $\Omega_{m2}$  are the critical densities for the energy densities  $\rho_r$ ,  $\rho_\Lambda$ ,  $\rho_{m1}$  and,  $\rho_{m2}$ , respectively with  $\Omega_r + \Omega_\Lambda + \Omega_{m1} + \Omega_{m2} = 1$ . The scale factor  $a$  and redshift  $z$  is related by the relation  $\frac{a_0}{a} = 1 + z$ , where we take  $a_0 = 1$ , consistent with the standard assumption of observational cosmology. In the dynamical system section, we probed the cosmic dynamics from the late-times perspectives and here we aim to study the observational perspectives of model using the low redshift data. Note that in present model, for the point  $E$ , one may have  $\rho_{m2} = \rho_{m20}a^{-9(1-\frac{1}{m})}$ . The cosmological phase of point  $E$  will be dominant during initial times. The stiff fluid satisfying  $p_s = \rho_s$  scales with  $\rho_s \propto a^{-6}$ . For the low redshift era, the fluid satisfying  $\rho = \rho_0 a^{-9+\delta}$  (for small  $\delta$ ) would decay faster than the stiff fluid satisfying  $\rho_s \propto a^{-6}$  and thus these components will be negligible during present times. So, we ignore this term containing  $\Omega_{m2}$  and write equation (66) in terms of redshift  $z$  as

$$H^2 = H_0^2 \left[ \Omega_{r0}(1+z)^4 + (1 - \Omega_{r0} - \Omega_{m1}) + \Omega_{m1}(1+z)^{\frac{-2(6m^2-8m+1)}{(2m-1)(m-1)}} \right] \quad (67)$$

Using Eq. (67), we constrain the model parameters involved in  $\omega_{eff}$  by using the Observational Hubble data [73] and Pantheon data [74]. Since, the radiation component of fluid is negligible during present times, we take the value of  $\Omega_r = 2.47 \times 10^{-5}$  [4].

The observational Hubble data (OHD) constitutes of 31 data points from the redshift range  $0.070 < z < 1.965$  [73]. The optimal values of the model parameters will be

determined by minimizing the  $\chi^2$  function, which is defined as follows [75, 76]

$$\chi_{OHD}^2(\theta) = \sum_{i=1}^{31} \frac{[H_{th}(\theta, z_i) - H_{obs}(z_i)]^2}{\sigma_{H(z_i)}^2} \quad (68)$$

where  $H_{th}(\theta, z_i)$  and  $H_{obs}(z_i)$  are the theoretical and observed values of the Hubble parameter  $H$ , respectively. Here,  $\theta = \{H_0, \Omega_{m1}, m\}$  be the parameter space and  $\sigma_{H(z_i)}^2$  be the standard deviation for the observed value of each  $H_{obs}(z_i)$ . The best fit Hubble parameter curve in comparison with the  $\Lambda$ CDM model have been given in Figure 8.

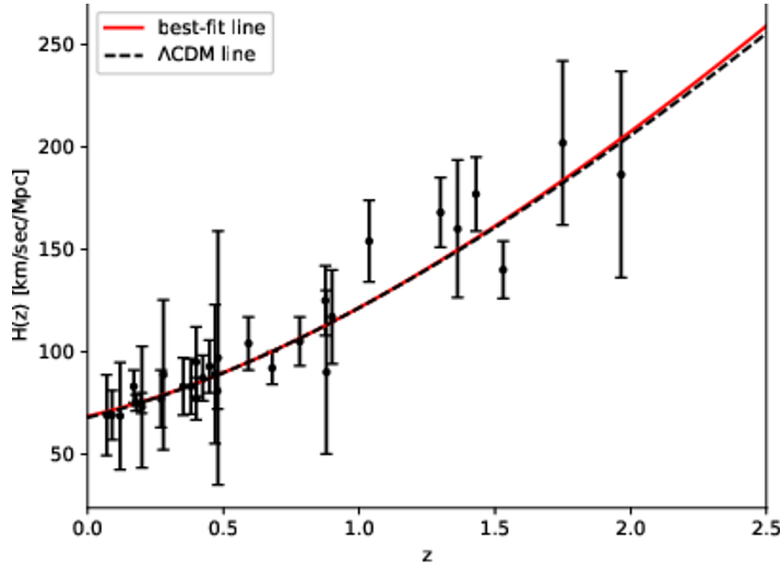


Figure 8: The best fit  $H(z)$  curve with OHD data and its error bars

We next use the the Pantheon sample consisting of 1048 SN Ia data compiled in Ref. [74] for the redshift range  $0.01 < z < 2.26$ . For the Pantheon data, the likelihood function  $\chi^2$  as:

$$\chi^2_{Pantheon} = \nabla \mu_i C_{ij}^{-1} \nabla \mu_j \quad (69)$$

where  $\nabla\mu_i \equiv \mu_{obs}(z_i) - \mu_{th}(z_i)$  and  $C_{ij}^{-1}$  is the inverse of total covariance matrix [74, 77]. The theoretically expected apparent magnitude  $\mu_{th}(z)$  is given by

$$\mu_{th}(z) = M + 5 \log_{10} [D_L(z)] + 5 \log_{10} \left[ \frac{c/H_0}{Mpc} \right] + 25 \quad (70)$$

where  $M$  is the absolute magnitude. The Hubble-free luminosity distance  $D_L(z)$  is defined by  $D_L(z) \equiv H_0(1+z) \int_0^z \frac{dz'}{H(z')}$  [78]. We may combine the parameters  $M$  and  $H_0$  to a new parameter  $\mathcal{M}$ , and rewrite the equation (70) as

$$\mu_{th}(z) = \mathcal{M} + 5 \log_{10} [D_L(z)] \quad (71)$$

where  $\mathcal{M} \equiv M + 5 \log_{10} \left[ \frac{c/H_0}{Mpc} \right] + 25$ . We employ the widely used Markov Chain Monte Carlo (MCMC) method to determine the best-fit values for the model parameters using *emcee* Python package developed by Foreman-Mackey et al. [79].

We minimize the  $\chi_{OHD}^2$  function and find the best fit values for  $H_0 = 67.8 \pm 4.0 \text{ km}/(s \cdot \text{Mpc})$ ,  $\Omega_{m1} = 0.40_{-0.32}^{+0.11}$  and  $m = -0.157_{-0.037}^{+0.150}$  with  $\chi_{min}^2 = 14.48$ .

We also use the OHD+Pantheon data to obtain the best fit values of  $H_0$ ,  $\Omega_{m1}$ ,  $m$ , and  $\mathcal{M}$  by minimizing the function  $\chi^2 = \chi_{OHD}^2 + \chi_{Pantheon}^2$ . The best fit values are  $H_0 = 68.8 \pm 1.9 \text{ km}/(s \cdot \text{Mpc})$ ,  $\Omega_{m1} = 0.286_{-0.073}^{+0.044}$ ,  $m = -0.156_{-0.049}^{+0.066}$  and  $\mathcal{M} = 23.808 \pm 0.012$  with  $\chi_{min}^2 = 1041.05$ . We plot the contour graph for parameters using the OHD+Pantheon data in Figure 9. A comparison of the best fit and  $1\sigma$  error values are given in Table 3.

| Parameters     | OHD                        | Pantheon+OHD               |
|----------------|----------------------------|----------------------------|
| $H_0$          | $67.8 \pm 4.0$             | $68.8 \pm 1.9$             |
| $\Omega_{m1}$  | $0.40_{-0.32}^{+0.11}$     | $0.286_{-0.073}^{+0.044}$  |
| $m$            | $-0.157_{-0.037}^{+0.150}$ | $-0.156_{-0.049}^{+0.066}$ |
| $\chi_{min}^2$ | 14.48                      | 1041.05                    |
| $\mathcal{M}$  | -                          | $23.808 \pm 0.012$         |

Table 3: Summary of the best fit values of model parameters, where  $H_0$  is in the units of  $\text{km}/(s \cdot \text{Mpc})$ .

The age of the universe may be given by  $t(z) = \int_z^\infty \frac{dz'}{(1+z')H(z')}$ . At the present times,  $z = 0$  may yield the age of universe  $t_0 = 13.49_{-0.45}^{+0.99}$  Gyr for the estimated value based on the OHD+Pantheon data within  $1\sigma$  error.

## 6 Statefinder diagnostic analysis

Dark energy properties can be explored in a model independent manner using the geometric parameters. The statefinder parameters involves the geometrical parameters such

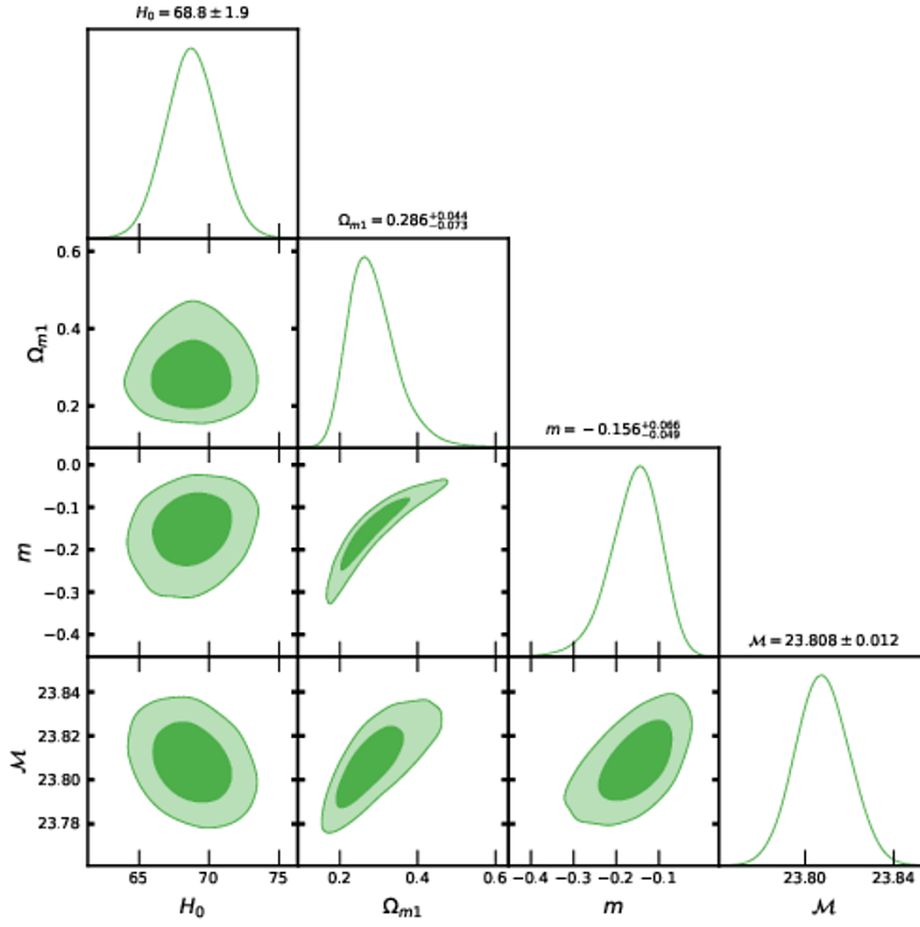


Figure 9:  $1\sigma - 2\sigma$  contour plots for the parameters  $\{H_0, \Omega_{m1}, m, \mathcal{M}\}$  using OHD+Pantheon data.

as the scale factor, Hubble parameters and its derivatives. The statefinder parameters  $\{r, s\}$  may be specified as [80]

$$r = 1 - 2(1+z)\frac{H'}{H} + (1+z)^2\frac{H''}{H} + (1+z)^2\left(\frac{H'}{H}\right)^2 \quad (72)$$

$$s = \frac{-2(1+z)\frac{H'}{H} + (1+z)^2\frac{H''}{H} + (1+z)^2\left(\frac{H'}{H}\right)^2}{3\left((1+z)\frac{H'}{H} - \frac{3}{2}\right)} \quad (73)$$

Whenever  $\{r, s\} = \{1, 0\}$  in the  $r - s$  plane, the model will resemble to the  $\Lambda$  Cold Dark Matter ( $\Lambda$ CDM) model, whereas, for  $\{r, s\} = \{1, 1\}$ , it will resemble to the the Standard Cold Dark Matter (SCDM) model. For the varying dark energy in a model, the value of  $r$  is not equal to 1. Within the  $r - s$  plane, the trajectories of the Chaplygin gas model and quintessence model fall into distinct domains. In particular, trajectories associated with the quintessence model traces path into regions characterized by  $r < 1$  and  $s > 0$ , whereas the Chaplygin gas model trajectories will belong to  $r > 1$  and  $s < 0$  region [80].

In the terms of dynamical system variables of the present model, the parameters  $r$  and  $s$  are given by

$$r = 3 - 9x_4 + 4x_4^2 - \frac{x_4x_6}{m-1} \quad (74)$$

$$s = \frac{2 - 9x_4 + 4x_4^2 - \frac{x_4x_6}{m-1}}{3\left(\frac{1}{2} - x_4\right)} \quad (75)$$

At critical point  $F$ , one may have  $\{r, s\} = \{1, 0\}$ , showing that the model demonstrates consistent alignment with the  $\Lambda$ CDM model. For point  $E$ ,  $\{r, s\} = \left\{\frac{m^2-9m+18}{m^2}, \frac{2m(m^2-9m+17)}{9(2-m)}\right\}$ . The values of the  $\{r, s\}$  parameters turn into  $\{1, 0\}$  when  $m = 2$ . In the same way, the  $\{r, s\}$  parameters at point  $G$  are expressed as  $\left\{\frac{(-2m^2+m+3)(-2m^2+m+1)}{(2m^2-3m+1)^2}, \frac{2(2-m)}{3(2m^2-3m+1)}\right\}$ . We use the effective Hubble parameter (67) of model to plot the behaviour of universe in the  $r - s$  plane, subjected to the best fit values from OHD+Pantheon data. The Fig. (10) highlights that the trajectory in the  $r - s$  plane would belong to Chaplygin gas models having  $r > 1$ ,  $s < 0$ .

## 7 Conclusions

In this study on  $f(R, \mathcal{G})$  model, we investigate the cosmic dynamics of universe where the dark matter and scalar field have been interacting to each other. The understanding of late stages of universe evolution have been studied by using dynamical system method in the modified gravity model defined by  $f(R, \mathcal{G}) = \alpha R^m + \beta \mathcal{G}^n$ , where  $m, n, \alpha$ , and  $\beta$  are parameters. This form of  $f(R, \mathcal{G})$  is admitted by the Noether symmetry analysis [72].

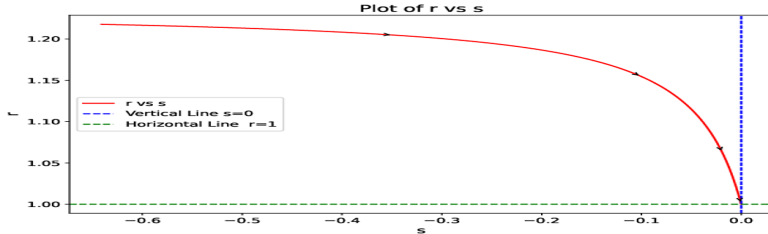


Figure 10: The  $r - s$  plane behaviour for central value of OHD+Pantheon best fit estimates.

We investigated the considered form of  $f(R, \mathcal{G})$  model with the flat FLRW spacetime and converts the cosmological system into an autonomous system. The eigenvalues of critical points are analysed for their stability nature. The dynamics of the universe's evolution are further explored through the investigation of the scale factor  $a$  and the deceleration parameter  $q$ . The critical point corresponding to the late-time accelerated expansion of the universe will exist in the model. This point is attracting in nature. In other words, an attractor will exist in model which signifies the de Sitter expansion of the universe.

The acceleration to deceleration phase transition may be explained in the model. The critical point corresponding to radiation phase will exist due to contribution from the terms of  $f(R, \mathcal{G})$  function. The critical point corresponding to matter dominated phase will depend on the model parameter  $m$ . For different parameter values, this point may have the quintessence or phantom evolution scenario also.

The effective equation of state parameter corresponding to critical points are utilized to write the effective Hubble parameter of the model. We use the low redshift data (such as OHD and Pantheon) to constrain the parameters involved in effective EoS parameter. The summary of constrained parameters have been presented in Table 3. The phase space between the parameters are obtained from the Markov chain Monte Carlo analysis and given in Fig. 9 for the OHD+Pantheon data. In summary, the resulting framework of model is consistent with these observations. We obtained the age of universe in model  $t_0 = 13.49^{+0.99}_{-0.45}$  Gyr. This aspect is also broadly consistent with the observations [4]. Apart from scrutinizing the phase space and observational aspects, we further scrutinize



the evolution of state-finder parameters to ascertain the intervals during which our model aligns with either  $\Lambda$  Cold Dark Matter( $\Lambda$ CDM) or Standard Cold Dark Matter (SCDM). In the  $r - s$  plane, the effective Hubble parameter of model reveals that the model will behave like Chaplygin gas models for the best fit values.

## Acknowledgement

We are grateful to the reviewers for comments which has been helpful in modification of the paper. Shivani, acknowledges CSIR-UGC, New Delhi, for the financial aid provided under the CSIR-UGC(JRF) scheme with Award Letter No. UGC-Ref.No.: 1332/(CSIR-UGC NET JUNE 2019). RC appreciates the financial assistance received from the ‘Incentive Grant’ through IoE, BHU.

## Data Availability

There are no new data associated with this article.

## References

- [1] S. Perlmutter et al. Measurements of  $\omega$  and  $\lambda$  from 42 high-redshift supernovae. *The Astrophysical Journal*, 517(2):565, 1999.
- [2] A G Riess et al. Observational evidence from supernovae for an accelerating universe and a cosmological constant. *The astronomical journal*, 116(3):1009, 1998.
- [3] J. Magana, M H Amante, M A Garcia-Aspeitia, et al. The cardassian expansion revisited: constraints from updated hubble parameter measurements and type ia supernova data. *Monthly Notices of the Royal Astronomical Society*, 476(1):1036–1049, 2018.
- [4] N Aghanim, Y Akrami, M Ashdown, et al. Planck 2018 results-vi. cosmological parameters. *Astronomy & Astrophysics*, 641:A6, 2020.
- [5] S Alam, M Ata, S Bailey, et al. The clustering of galaxies in the completed sdss-iii baryon oscillation spectroscopic survey: cosmological analysis of the dr12 galaxy sample. *Monthly Notices of the Royal Astronomical Society*, 470(3):2617–2652, 2017.
- [6] Planck Collaboration, PAR Ade, N Aghanim, et al. Planck 2013 results. xvi. cosmological parameters. *A&A*, 571:A16, 2014.

- [7] P A R Ade, N Aghanim, M Arnaud, et al. Planck 2015 results-xiii. cosmological parameters. *Astronomy & Astrophysics*, 594:A13, 2016.
- [8] M E A Betoule, R Kessler, J Guy, et al. Improved cosmological constraints from a joint analysis of the sdss-ii and snls supernova samples. *Astronomy & Astrophysics*, 568:A22, 2014.
- [9] S Weinberg. The cosmological constant problem. *Reviews of modern physics*, 61(1):1, 1989.
- [10] T Padmanabhan. Cosmological constant—the weight of the vacuum. *Physics reports*, 380(5-6):235–320, 2003.
- [11] A Padilla. Lectures on the cosmological constant problem. *arXiv preprint arXiv:1502.05296*, 2015.
- [12] L Perivolaropoulos. Six puzzles for lcdm cosmology. *arXiv preprint arXiv:0811.4684*, 2008.
- [13] Y L Bolotin, A Kostenko, O A Lemets, et al. Cosmological evolution with interaction between dark energy and dark matter. *International Journal of Modern Physics D*, 24(03):1530007, 2015.
- [14] B Wang, E Abdalla, F Atrio-Barandela, et al. Dark matter and dark energy interactions: theoretical challenges, cosmological implications and observational signatures. *Reports on Progress in Physics*, 79(9):096901, 2016.
- [15] C van de Bruck and J Morrice. Disformal couplings and the dark sector of the universe. *Journal of Cosmology and Astroparticle Physics*, 2015(04):036, 2015.
- [16] C G Boehmer, N Tamanini, and M Wright. Interacting quintessence from a variational approach. i. algebraic couplings. *Physical Review D*, 91(12):123002, 2015.
- [17] J Gleyzes, D Langlois, M Mancarella, et al. Effective theory of interacting dark energy. *Journal of Cosmology and Astroparticle Physics*, 2015(08):054, 2015.
- [18] G D’Amico, T Hamill, and N Kaloper. Quantum field theory of interacting dark matter and dark energy: Dark monodromies. *Physical Review D*, 94(10):103526, 2016.
- [19] S Pan, G S Sharov, and W Yang. Field theoretic interpretations of interacting dark energy scenarios and recent observations. *Physical Review D*, 101(10):103533, 2020.

- [20] S Chatzidakis, A Giacomini, P G L Leach, et al. Interacting dark energy in curved flrw spacetime from weyl integrable spacetime. *Journal of High Energy Astrophysics*, 36:141–151, 2022.
- [21] A Singh and S Krishnannair. Varying vacuum models with spatial curvature: a dynamical system perspective. *General Relativity and Gravitation*, 56(02):31, 2024.
- [22] M Gavela, D Hernandez, L L Honorez, et al. Dark coupling. *Journal of Cosmology and Astroparticle Physics*, 2009(07):034, 2009.
- [23] Y Wang, D Wands, G-B Zhao, et al. Post-planck constraints on interacting vacuum energy. *Physical Review D*, 90(2):023502, 2014.
- [24] W Yang, O Mena, S Pan, et al. Dark sectors with dynamical coupling. *Physical Review D*, 100(8):083509, 2019.
- [25] W Yang, E Di Valentino, O Mena, and S Pan. Dynamical dark sectors and neutrino masses and abundances. *Physical Review D*, 102(2):023535, 2020.
- [26] Y-H Li and X Zhang. Running coupling: does the coupling between dark energy and dark matter change sign during the cosmological evolution? *The European Physical Journal C*, 71:1–9, 2011.
- [27] S Nojiri and S D Odintsov. Unified cosmic history in modified gravity: from  $f(r)$  theory to lorentz non-invariant models. *Physics Reports*, 505(2-4):59–144, 2011.
- [28] V Faraoni and S Capozziello. *Beyond Einstein gravity: A Survey of gravitational theories for cosmology and astrophysics*. Springer, 2011.
- [29] A Dobado and A L Maroto. Inflatonless inflation. *Physical Review D*, 52(4):1895, 1995.
- [30] G Dvali, G Gabadadze, and M Porrati. 4d gravity on a brane in 5d minkowski space. *Physics Letters B*, 485(1-3):208–214, 2000.
- [31] J B Jimenez and A L Maroto. Cosmological evolution in vector-tensor theories of gravity. *Physical Review D*, 80(6):063512, 2009.
- [32] S Nojiri and S D Odintsov. Modified  $f(R)$  gravity consistent with realistic cosmology: From a matter dominated epoch to a dark energy universe. *Physical Review D*, 74(8):086005, 2006.

- [33] E Elizalde and D Sáez-Gómez.  $f(R)$  cosmology in the presence of a phantom fluid and its scalar-tensor counterpart: Towards a unified precision model of the evolution of the universe. *Physical Review D*, 80(4):044030, 2009.
- [34] J A R Cembranos. Dark matter from  $R^2$  gravity. *Physical review letters*, 102(14):141301, 2009.
- [35] S Nojiri and S D Odintsov. Modified gravity with  $\ln r$  terms and cosmic acceleration. *General Relativity and Gravitation*, 36:1765–1780, 2004.
- [36] P K S Dunsby, E Elizalde, R Goswami, et al.  $\lambda$  cdm universe in  $f(r)$  gravity. *Physical Review D*, 82(2):023519, 2010.
- [37] V Faraoni.  $f(R)$  gravity: successes and challenges. *arXiv preprint arXiv:0810.2602*, 2008.
- [38] A De la Cruz-Dombriz and A Dobado.  $f(R)$  gravity without a cosmological constant. *Physical Review D*, 74(8):087501, 2006.
- [39] W Hu and I Sawicki. Models of  $f(R)$  cosmic acceleration that evade solar system tests. *Physical Review D*, 76(6):064004, 2007.
- [40] F G Alvarenga, A de la Cruz-Dombriz, M J S Houndjo, M E Rodrigues, and D Saez-Gomez. Dynamics of scalar perturbations in  $f(r, t)$  gravity. *Physical Review D*, 87(10):103526, 2013.
- [41] H Shabani and M Farhoudi.  $f(r, t)$  cosmological models in phase space. *Physical Review D*, 88(4):044048, 2013.
- [42] E H Baffou, A V Kpadonou, M E Rodrigues, M J S Houndjo, and J Tossa. Cosmological viable  $f(r, t)$  dark energy model: dynamics and stability. *Astrophysics and Space Science*, 356(1):173–180, 2015.
- [43] S Nojiri, S D Odintsov, and S Ogushi. Friedmann–robertson–walker brane cosmological equations from the five-dimensional bulk (a) d s black hole. *International Journal of Modern Physics A*, 17(32):4809–4870, 2002.
- [44] A De Felice and S Tsujikawa. Construction of cosmologically viable  $f(G)$  gravity models. *Physics Letters B*, 675(1):1–8, 2009.
- [45] S Nojiri, S D Odintsov, and P V Tretyakov. From inflation to dark energy in the non-minimal modified gravity. *Progress of Theoretical Physics Supplement*, 172:81–89, 2008.

- [46] K Bamba, S D Odintsov, L Sebastiani, et al. Finite-time future singularities in modified Gauss–Bonnet and  $f(R, G)$  gravity and singularity avoidance. *The European Physical Journal C*, 67:295–310, 2010.
- [47] S D Odintsov, V K Oikonomou, and S Banerjee. Dynamics of inflation and dark energy from  $f(R, G)$  gravity. *Nuclear Physics B*, 938:935–956, 2019.
- [48] A De la Cruz-Dombriz and D Sáez-Gómez. On the stability of the cosmological solutions in  $f(R, G)$  gravity. *Classical and Quantum Gravity*, 29(24):245014, 2012.
- [49] S S Da Costa, F V Roig, J S Alcaniz, et al. Dynamical analysis on  $f(R, G)$  cosmology. *Classical and Quantum Gravity*, 35(7):075013, 2018.
- [50] M M Ivanov and A V Toporensky. Cosmological dynamics of fourth-order gravity with a gauss-bonnet term. *Gravitation and Cosmology*, 18(1):43–53, 2012.
- [51] S V Lohakare, K Rathore, and B Mishra. Observational constrained  $f(r, g)$  gravity cosmological model and the dynamical system analysis. *Classical and Quantum Gravity*, 40(21):215009, 2023.
- [52] K F Dialektopoulos, J L Said, and Z Oikonomopoulou. Dynamical systems in einstein gauss-bonnet gravity. *arXiv:2211.06076v1 [gr-qc]*, 2022.
- [53] S D Odintsov and V K Oikonomou. Autonomous dynamical system approach for  $f(R)$  gravity. *Physical Review D*, 96(10):104049, 2017.
- [54] P Shah, G C Samanta, and S Capozziello. Qualitative behavior of cosmological models combining various matter fields. *International Journal of Modern Physics A*, 33(18n19):1850116, 2018.
- [55] M Hohmann, L Järv, and U Ualikhanova. Dynamical systems approach and generic properties of  $f(T)$  cosmology. *Physical Review D*, 96(4):043508, 2017.
- [56] A Singh. Homogeneous and anisotropic cosmologies with affine eos: a dynamical system perspective. *European Physical Journal C*, 83(8):696, 2023.
- [57] E J Copeland, A R Liddle, and D Wands. Exponential potentials and cosmological scaling solutions. *Physical Review D*, 57(8):4686, 1998.
- [58] R Raushan, S Angit, and R Chaubey. Linear and center manifold analysis of frw cosmological model with variable equation of state in lyra geometry. *The European Physical Journal Plus*, 136(4):440, 2021.

- [59] R Raushan and R Chaubey. Finsler–randers cosmology in the framework of a particle creation mechanism: a dynamical systems perspective. *The European Physical Journal Plus*, 135(2):228, 2020.
- [60] R Raushan, A K Shukla, R Chaubey, and T Singh. Locally rotationally symmetric bianchi type-i cosmological model with dynamical  $\lambda$  and  $g$  in  $f(R)$  gravity. *Pramana*, 92:1–9, 2019.
- [61] R Raushan and R Chaubey. Dynamical analysis of anisotropic cosmological model with quadratic dark sector coupling. *International Journal of Geometric Methods in Modern Physics*, 16(02):1950023, 2019.
- [62] A Singh, G P Singh, and A Pradhan. Cosmic dynamics and qualitative study of rastall model with spatial curvature. *International Journal of Modern Physics A*, 37(16):2250104, 2022.
- [63] A Singh. Qualitative study of lyra cosmologies with spatial curvature. *Chinese Journal of Physics*, 79:481–489, 2022.
- [64] A Singh. Qualitative aspects of kantowski-sachs cosmologies with cosmological constant and stiff fluid. *European Physical Journal Plus*, 138(03):188, 2023.
- [65] A Singh, A K Shukla, and S Krishnannair. Cosmic dynamics of isotropic models with inhomogeneous eos: a dynamical system perspective. *International Journal of Modern Physics A*, 38(31):2350169, 2023.
- [66] A Singh. Lyra cosmologies with the dynamical system perspective. *Physica Scripta*, 99(4):045011, 2024.
- [67] G F R Ellis and J Wainwright. *Dynamical systems in cosmology*. Cambridge University Press, 1997.
- [68] A A Coley. *Dynamical systems and cosmology*, volume 291. Springer Science & Business Media, 2003.
- [69] S Bahamonde, C G Bohmer, S Carloni, E J Copeland, W Fang, and N Tamanini. Dynamical systems applied to cosmology: Dark energy and modified gravity. *Physics Reports*, 775–777:1–122, 2018.
- [70] E J Copeland, M Sami, and S Tsujikawa. Dynamics of dark energy. *International Journal of Modern Physics D*, 15(11):1753–1935, 2006.

- [71] A Singh. Dynamical systems of modified gauss-bonnet gravity: cosmological implications. *arXiv:2405.07546v1[gr-qc]*, 2024.
- [72] F Bajardi and R D’Agostino. Late-time constraints on modified gauss-bonnet cosmology. *General Relativity and Gravitation*, 55(3):49, 2023.
- [73] G S Sharov and V O Vasiliev. How predictions of cosmological models depend on hubble parameter data sets. *Mathematical Modelling and Geometry*, 6(1):1–20, 2018.
- [74] D M Scolnic et al. The complete light-curve sample of spectroscopically confirmed SNe Ia from pan-STARRS1 and cosmological constraints from the combined pantheon sample. *The Astrophysical Journal*, 859(2):101, 2018.
- [75] S Mandal, A Singh, and R Chaubey. Observational constraints and cosmological implications of nle model with variable g. *The European Physical Journal Plus*, 137(11), 2022.
- [76] S Mandal, A Singh, and R Chaubey. Cosmic evolution of holographic dark energy in f(q,t) gravity. *International Journal of Geometric Methods in Modern Physics*, 20(05):2350084, 2023.
- [77] K Asvesta, L Kazantzidis, L Perivolaropoulos, and C G Tsagas. Observational constraints on the deceleration parameter in a tilted universe. *Monthly Notices of the Royal Astronomical Society*, 513(2):2394–2406, 2022.
- [78] S Mandal, A Singh, and R Chaubey. Late-time constraints on barotropic fluid cosmology. *Physics Letters A*, 519:129714, 2024.
- [79] D Foreman-Mackey, D W Hogg, D Lang, and J Goodman. *emcee*: The MCMC hammer. *Publications of the Astronomical Society of the Pacific*, 125(925):306–312, 2013.
- [80] V Sahni, T D Saini, A A Starobinsky, et al. Statefinder—a new geometrical diagnostic of dark energy. *Journal of Experimental and Theoretical Physics Letters*, 77:201–206, 2003.